Atmos. Meas. Tech., 5, 1925–1934, 2012
www.atmos-meas-tech.net/5/1925/2012/
doi:10.5194/amt-5-1925-2012

Atmospheric Measurement Techniques

Performance of a low-cost methane sensor for ambient concentration measurements in preliminary studies

W. Eugster[1] **and G. W. Kling**[2]

[1]ETH Zurich, Institute of Agricultural Sciences, Universitätsstrasse 2, 8092 Zurich, Switzerland
[2]University of Michigan, Department of Ecology & Evolutionary Biology, Ann Arbor, MI 48109-1048, USA

Correspondence to: W. Eugster (eugsterw@ethz.ch)

Received: 29 February 2012 – Published in Atmos. Meas. Tech. Discuss.: 30 March 2012
Revised: 5 July 2012 – Accepted: 17 July 2012 – Published: 13 August 2012

Abstract. Methane is the second most important greenhouse gas after CO_2 and contributes to global warming. Its sources are not uniformly distributed across terrestrial and aquatic ecosystems, and most of the methane flux is expected to stem from hotspots which often occupy a very small fraction of the total landscape area. Continuous time-series measurements of CH_4 concentrations can help identify and locate these methane hotspots. Newer, low-cost trace gas sensors such as the Figaro TGS 2600 can detect CH_4 even at ambient concentrations. Hence, in this paper we tested this sensor under real-world conditions over Toolik Lake, Alaska, to determine its suitability for preliminary studies before placing more expensive and service-intensive equipment at a given locality. A reasonably good agreement with parallel measurements made using a Los Gatos Research FMA 100 methane analyzer was found after removal of the strong sensitivities for temperature and relative humidity. Correcting for this sensitivity increased the absolute accuracy required for in-depth studies, and the reproducibility between two TGS 2600 sensors run in parallel is very good. We conclude that the relative CH_4 concentrations derived from such sensors are sufficient for preliminary investigations in the search of potential methane hotspots.

1 Introduction

Although methane concentrations are much lower than those of carbon dioxide in the atmosphere, it is still the second most important greenhouse gas because its greenhouse warming potential is 20–25 times greater than that of CO_2. In addition, CH_4 is more dynamic than CO_2 in part because its lifetime in the atmosphere is on the order of 10–12 yr, much shorter than that of CO_2. While steady increases of CH_4 in the atmosphere contribute to global warming, its sources are not uniformly distributed across terrestrial and aquatic ecosystems; often the highest methane fluxes come from localized hotspots, which may occupy only a very small area of the total landscape. In addition, recent scientific debates have centered on how CH_4 dynamics may accelerate future global warming through feedback mechanisms, especially related to the warming of arctic ecosystems (Serreze and Francis, 2006; McGuire et al., 2006).

In the Arctic, such hotspots are generally associated with wetlands or shallow waters where sedge species with aerenchyma vent methane produced in the anoxic sediments to the atmosphere (Reeburgh et al., 1998). Lakes can be hotspots of methane emissions under certain circumstances during turnover or mixing events (Eugster et al., 2003). Often, large methane fluxes from lakes are associated with ebullition (DelSontro et al., 2010; Eugster et al., 2011); in the Arctic this is easily visible during the cold season thanks to bubbles trapped in the ice (Walter et al., 2006). One approach to find hotspots is to move a gas analyzer across the landscape and observe the concentration changes in the near-surface atmosphere that can be associated with a point source of methane emissions. So far, this was mostly done with sensors carried by helicopter (e.g., Karapuzikov et al., 1999; Zirnig et al., 2004; Dzikowski et al., 2009; Haifang et al., 2011), by small aircraft (e.g., Hiller et al., 2011), by ground based laser scanning (e.g., Gibson et al., 2006) or surface surveying with a field-portable flame-ionization detector (e.g., Schroth et al., 2012). All these approaches, however, fail if such hotspots are not constantly emitting methane. In

such cases, a random walk survey may leave a misleading picture if the temporal dynamics of the methane emissions are unknown.

This is specifically the case in arctic lakes, where methane is expected to be produced in the anoxic lake bottom sediments. Due to thermal stratification of the waters (warmer waters on top of cold bottom waters), even high methane production at the bottom may not automatically lead to high emissions at the lake surface due to lack of mixing in the lake. Hence, a systematic sampling over longer time periods is essential to quantitatively measure the potentially short periods of high methane emissions during specific mixing or turnover events (e.g., as caused by cold front passages; MacIntyre et al., 2009). Similarly, it has been shown for soil N_2O fluxes that careful consideration of spatial autocorrelation is necessary to obtain a representative flux estimate from a given area (Folorunso and Rolston, 1984).

Such systematic sampling measurements are still rather costly, and hence we carried out a field experiment with a low-cost solid-state sensor that recently appeared on the market, to explore its suitability for preliminary studies that aim to find locations where episodic high CH_4 effluxes would justify the investment for an in-depth study with state-of-the-art gas analyzers. Low cost in this context means that the solid-state sensor alone costs less than € 40. A rough calculation of the scalar footprint (Schmid, 1994) for a concentration measurement made with a low-cost sensor at 1 m above ground level in the arctic moist acidic tussock tundra (with a roughness length of 5.6 ± 0.9 cm; see Eugster et al., 2005) suggests that such a sensor should show a response to hotspots within ca. 1300 m upwind under neutral atmospheric stratification. Hence, it is envisaged that with an appropriate sampling design such low-cost sensors could be placed in a regular grid with ≈ 1 km spacing to identify times, duration, and approximate locality of hotspots at the landscape scale.

2 Material and methods

2.1 The TGS 2600 gas sensor

The Taguchi Gas Sensor (TGS) 2600 (Figaro Engineering Inc., Osaka, Japan) is a low-power consumption high-sensitivity gas sensor for the detection of air contaminants such as those typical for cigarette smoke (Figaro, 2005a). The general field of application of TGS sensors is leak detectors of toxic and explosive gases (Figaro, 2005b). In the case of methane, the risk of explosion starts at concentrations around 4.4 %, which is orders of magnitude higher than ambient concentrations around 1.8 ppm (Forster et al., 2007), and hence such solid-state sensors were not sensitive enough for measurements in ambient air. For example, Wong et al. (1996) reported on earlier TGS sensors that showed almost negligible change in response to non-polar gases such as hydrogen and methane. A few years later, Brudzewski (1998) reported that an older TGS 813 reacted to pulses of air and methane ranging between 1600 ppm and 4000 ppm, but not at ambient concentrations (≈ 1.8 ppm). Also, the NGM 2611 methane sensor used by Tümer and Gündüz (2010) is only sensitive to CH_4 in the range 1000–10 000 ppm. To the best of our knowledge, the TGS 2600 is the first sensor for which the manufacturer indicates a sensitivity to methane even in the ppm range (Fig. 1a). Besides methane, a sensitivity to carbon monoxide, iso-butane, ethanol and hydrogen is reported by the manufacturer (Figaro, 2005a).

In addition, Kotarski et al. (2011) report a successful application to detect scents of lemon, musk, pine, and melissa. Ferri et al. (2009a) reported that their tests with the TGS 2600 were in good agreement with the manufacturer's datasheet (Figaro, 2005a), and they also confirm a good time response of the sensor to prescribed variations in H_2 concentrations in the air. Additional laboratory tests were carried out by De Marcellis et al. (2009) and Morsi (2007, 2008), but no field deployments have been made to test the sensor's performance and suitability for preliminary studies. We use this terminology explicitly to specify that we do not expect such a low-cost multi-gas sensor to provide the basis for studies that require accurate and precise concentration information, but we do expect a potential for suitable use in preliminary studies such as described above.

2.2 Principle of operation

The TGS sensors are solid-state sensors mounted in a TO5 package containing a metal oxide as the sensing material, such as SnO_2 (Figaro, 2005b). According to Ferri et al. (2009b), however, the metal oxide used for the TGS 2600 sensor is TiO_2. This metal oxide, in the form of granular micro-crystals, is heated to a high temperature at which oxygen in the air is adsorbed to the crystal surface (Figaro, 2005b). In this configuration the sensor has a certain resistance R_0 in clean air, which is reduced under the presence of a gas to which the TGS sensor is sensitive. This reduced resistance R_s can be expressed by a power function (Figaro, 2005b):

$$R_s = A[C]^{-\alpha} , \quad (1)$$

where R_s is the actual sensor resistance, A is a coefficient for the gas at concentration $[C]$, and α is the slope of the curve as shown in Fig. 1a. For the application in this study, we measured R_s in a simple electronic circuit where the voltage drop over a precision resistor R_L in series with R_s was measured (Fig. 2).

From such a set-up, the sensor resistance can be determined as (Figaro, 2005a):

$$R_s = \frac{V_c \times R_L}{V_{out}} - R_L , \quad (2)$$

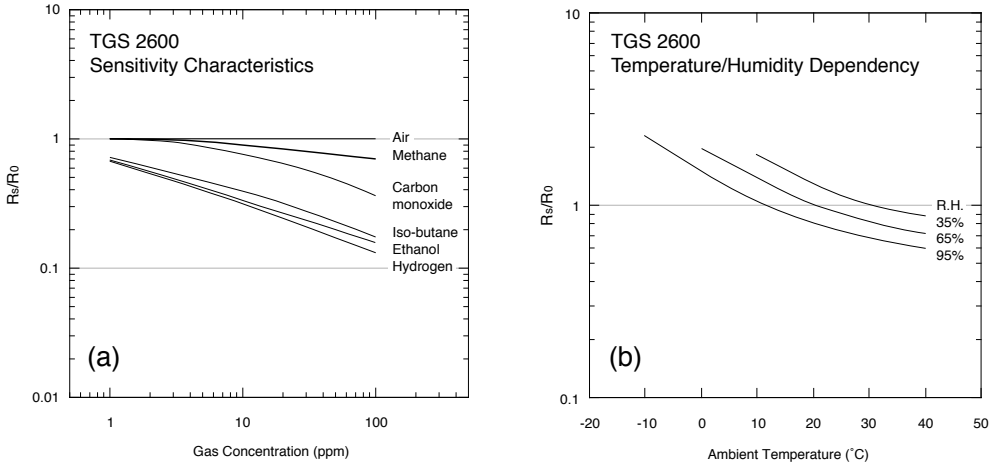

Fig. 1. General Figaro TGS 2600 sensor response **(a)** and sensitivity to temperature and relative humidity **(b)** according to manufacturer specifications. R_S/R_0 is the ratio between sensor resistance (R_S) under presence of a specific component in relation to the reference resistance (R_0) in "fresh" air without any of the additional chemical components. Modified from Figaro (2005a).

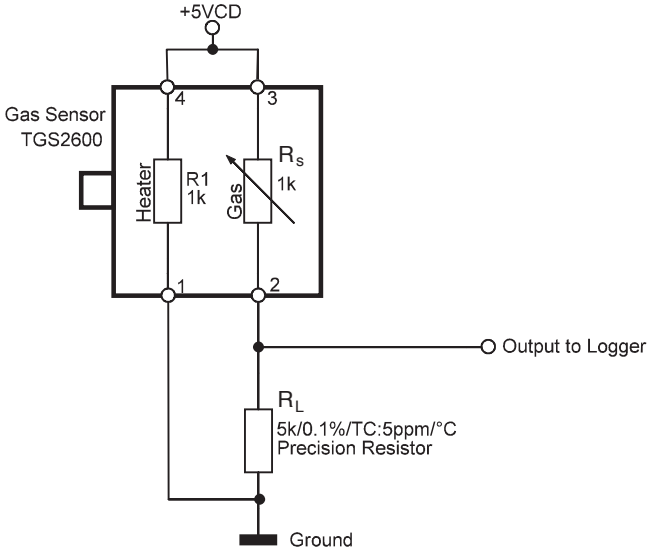

Fig. 2. Sensor configuration used in this study. The variable sensor resistance R_S was measured between pins 2 and 3 and converted to a measurable voltage using an $R_L = 5\,\mathrm{k}\Omega$ precision resistor.

where V_c is the supply voltage of 5.0 V DC, and V_{out} is the voltage measured over the precision resistor R_L. Finally, the ratio between the actual sensor resistance R_S and the clean-air resistance R_0 is the sensor signal of interest to deduce methane concentrations (Fig. 1).

The main problem to overcome is the sensor's sensitivity to ambient temperature and relative humidity (Fig. 1b), for which only an empirical approach for correction is suggested by the manufacturer (Figaro, 2005b) which includes three steps: (1) identify the range of ambient temperature and humidity expected in the application, (2) obtain sensitivity curves for the target gas, and (3) apply a correction to approximate the average curve. Because this sensor is a multi-gas sensor primarily used in cigarette smoke detectors, there is a multitude of potential cross-sensitivities to gases other than CH_4; this aspect will be discussed in detail in Sect. 4.

2.3 Data acquisition and ancillary measurements

The TGS 2600 sensor signals were recorded by a Campbell Scientific CR3000 data logger, which also measured temperature and relative humidity using a Campbell Scientific sensor model CS215-L12. Its temperature sensor has an accuracy of ±0.4 K over the range +5 to +40 °C, which increases to ±0.9 K over the full measurement range −40 to +70 °C. Relative humidity is accurate to within ±2 % in the range 10–90 %, and increases to ±4 % at the extremes of the range. Atmospheric pressure was measured with a Vaisala PTB110 barometer with an uncertainty of ±0.15 hPa. Laboratory tests were carried out with a Campbell Scientific CR510 data logger, both using a single-ended measurement that resolves voltage signals with 666 µV resolution in the range ±2500 mV, and using a differential voltage reading in the range ±250 mV with a resolution of 33.3 µV relative to a 1150 mV reference signal. Test measurements were carried out every 5 s and stored in the internal memory. In the field, measurements were carried out every 10 s from which 1-min averages were computed and stored on the data logger's CF card.

2.4 CH_4 reference measurements

Field measurements with two TGS 2600 were made in parallel with a Los Gatos Research (Mountain View, CA, USA) Fast Methane Analyzer (FMA-100, serial number 09-0057) on a moored floating platform on Toolik Lake, Alaska (68°37′52″ N, 149°36′10″ W, 720 m a.s.l.). The primary

purpose of this analyzer was to measure methane fluxes from the lake with the eddy covariance method (Eugster and Plüss, 2010). Air was drawn through the analyzer by a Varian 600 Tri Scroll pump, and data were digitally recorded at 20 Hz, from which 1 min averages were computed for comparison with the TGS 2600 measurements. In addition, the analog output of the FMA-100 was also recorded on the CR3000 data logger to allow the synchronization of the digital data from the FMA-100 with the analog TGS 2600 data. The FMA-100 is an integrated off-axis cavity ringdown spectrometer working at a cell pressure around 138 Torr. The instrument used here (model number 908-0001-0003, serial number 09-0057) has a minimum noise level of 0.26 ppb (1.4 ppb for 1 s integration times) as determined from Allan variance analysis (Werle, 2010). Its suitability for high-quality atmospheric concentration and flux measurements has been demonstrated by Eugster and Plüss (2010) and Tuzson et al. (2010), among others. Concentration calibration checks were always within the uncertainty of the calibration tank available at Toolik Field Station (1.894 ppm ±5 %).

2.5 Uncertainty assessment

The uncertainty in CH_4 concentrations that are a result of inaccuracies in the measurements of air temperature and relative humidity are assessed via bootstrapping (Efron, 1979) using the boot procedure of the R statistical software (R Development Core Team, 2010). We chose a parametric bootstrapping approach in which we simulated (a) random uncertainties in both temperature and relative humidity specified by a normal distribution with mean zero and standard deviation according to sensor specifications given above, and (b) systematic deviations of ±4 K in temperature and/or ±5 % in relative humidity. Relative humidity was kept within the boundaries of 0 to 100 %, whereas no limits were set for temperature perturbations. Bootstrapping statistics were obtained from 500 replications.

3 Results

The relevant measurement signal is the ratio between the sensor resistance under presence of methane and other trace gases (R_s) in relation to the sensor resistance under absence of these gases (R_0). All attempts to directly use the voltage signal from the sensor as a measure for CH_4 concentration failed because in such a simple approach only ≈ 1 % of the total variance was due to methane. Successful, however, was the approach to first convert all measured V_{out} voltage signals to sensor resistances R_s according to Eq. (2). We used a precision resistor $R_L = 5\,k\Omega$ and a stabilized supply voltage V_c of 5.0 V DC (Fig. 2).

Next we quantified the reference resistance R_0 that would result from clean-air measurements without CH_4. In principle, this should be feasible with artificial gas mixtures, but as can be seen in Fig. 1b, there is such a strong dependence on temperature and relative humidity that it is not surprising that dry gas standards cannot be used. The manufacturer consequently defined $R_s/R_0 = 1$ for a relative humidity of 65 % and a temperature of 20 °C (Figaro, 2005a, see also Fig. 1b). This means that the sensor must be considered a relative indicator for CH_4 concentrations, and hence we can simply replace R_0 by the minimum R_s that we find in our data. Hence, we set R_0 to the sensor resistance at background levels of CH_4 at the given temperature and relative humidity that existed when this minimum R_0 was observed. This means that we obtain $R_s/R_0 \geq 1$ by definition, which is similar to what the manufacturer specifies, but with an offset to allow us to relate sensor output to absolute concentrations.

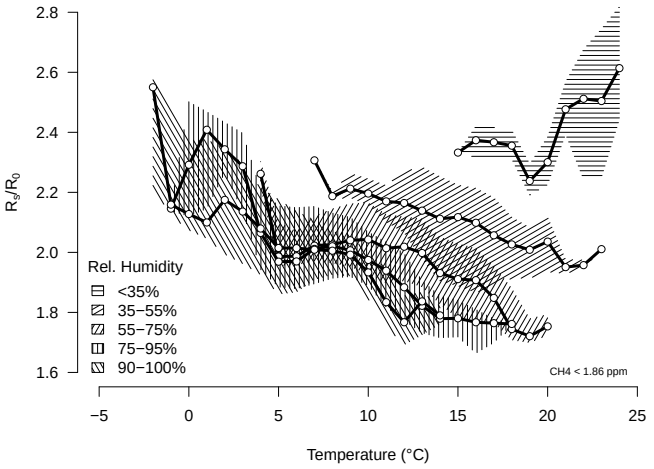

Fig. 3. Observed sensor sensitivity to ambient temperature and relative humidity at CH_4 concentrations < 1.86 ppm during the full 2011 field season at Toolik Lake. At relative humidities ≥ 35 %, the sensor resistance ratio follows the expected curves in Fig. 1b with an offset, but if the air is too dry (relative humidity < 35 %), the sensor does not provide reliable data that could be used to quantify CH_4 concentrations. Each curve and shaded area shows the binned median and interquartile range, respectively, of the selected range of relative humidities (see legend). Temperature bins were chosen 2 °C wide with 50 % overlap.

3.1 Sensitivity to relative humidity and temperature

Figure 3 shows the dependence of R_s/R_0 on temperature and relative humidity for the whole field season 2011, which generally follows the expected pattern for relative humidity ranging between 35 and 100 %. At relative humidity below 35 %, however, the sensor no longer obeyed the general rule that shows decreasing R_s/R_0 with increasing temperatures if relative humidity was kept in a narrow range (that is, 16–35 % in our case). That the manufacturer does not mention how the sensor should behave at relative humidity below 35 % (see Fig. 1b) is an indication that the sensor does not provide reliable information at lower atmospheric moisture levels, and

our experience suggests that even at 35 % relative humidity the sensor response is not as predictable as the manufacturer specifies. We excluded conditions with relative humidity < 40 % from further analysis.

To determine which factors actually influence the sensor signal, we carried out an analysis of variance using R_s/R_0 as the response variable, and methane concentration, linear trend of the sensor signal over time, relative humidity and air temperature as predictor variables (Table 1). This analysis indicated that over the full season 2011 more than one third (36 %) of the variance is simply attributable to the linear trend of the sensor signal, and the expected temperature and relative humidity accounted for another 34 % of the variance. This means that random variations in methane concentrations are only responsible for 18 % of the signal variation seen in our time series.

Although the linear trend is most important, it is essential for practical reasons to first correct for relative humidity and temperature effects, after which the corrected R_s/R_0 can be translated to methane concentrations. Once the translation is complete, the linear trend associated with the instrument drift (and not with the true seasonal trend) can be removed in a last step. Using this procedure would simplify the calibration requirements; it would be sufficient to take an air sample at the beginning and at the end of a deployment period (e.g., as long as one season according to results from our field experiment), analyze these samples by standard gas chromatography or laser absorption spectroscopy, and use the two calibration points for removal of the temporal trend.

3.2 Removing relative humidity and temperature sensitivities

In order to estimate one single correction algorithm for the TGS 2600 sensors in general, we used the information in Fig. 1b, digitized the curves in 10 °C intervals, and then fitted the following trend surface to the manufacturer's specification:

$$\frac{R_0}{R_s} = (0.024 \pm 0.032) + (0.0072 \pm 0.0004) \cdot \mathrm{rH} + (0.0246 \pm 0.0007) \cdot T_a \,, \quad (3)$$

($n = 11$, adjusted $R^2 = 0.9913$) with rH relative humidity in percent, and T_a air temperature in °C. To test whether this approximation can be used for our sensors, we used an iterative procedure to remove the offset in R_s/R_0 as we defined it, and then obtained best fits for the rH and T_a terms for an intercept that matches the one in Eq. (3). This yielded adjusted R^2 of 0.6337 and 0.7425 for sensors 1 and 2, respectively. The coefficients for rH were 0.0085 ± 0.0004 and 0.0076 ± 0.0003, and those for T_a were 0.0408 ± 0.0014 and 0.0369 ± 0.0010 for sensors 1 and 2, respectively. This shows that there are some differences in individual sensors that must be kept in mind, but for the purpose of using this sensor as a proxy for CH_4 concentrations in preliminary studies, this is acceptable.

To remove the contribution of rH and T_a from our R_s/R_0 signals, we must recall that we used a hyperbolic approach in Eq. (3), and that the relevant information is not the absolute signal but its ratio relative to clean air at the same temperature and humidity. Hence, we remove rH and T_a by computing a corrected ratio $(R_s/R_0)_{corr}$:

$$\left(\frac{R_s}{R_0}\right)_{corr} = \frac{R_s}{R_0} \cdot (0.024 + 0.0072 \cdot \mathrm{rH} + 0.0246 \cdot T_a) \,. \quad (4)$$

3.3 Conversion to CH_4 concentrations

As already mentioned, it is only practical to remove the linear trend in our data if we can compare methane information obtained from an independent sample with our sensor data; with this independent information we can convert our ratio of resistances to ppm CH_4. Using a linear regression approach with our reference CH_4 concentrations from the FMA, we obtained the following equation to convert our signal to $[CH_4]_{raw}$:

$$[CH_4]_{raw} = (1.8280 \pm 0.0005) + (0.0288 \pm 0.0002) \cdot \left(\frac{R_s}{R_0}\right)_{corr} \,. \quad (5)$$

For the sake of simplicity, we start with an offset of 1.8 and a multiplier of 0.1 for a given sensor for which we have no better calibration yet, $[CH_4]_{raw} \approx 1.8 + 0.1 \cdot (R_s/R_0)_{corr}$, and then apply a calibration as described in what follows.

3.4 Calibrating CH_4 concentrations

To simulate a typical field experiment where there is no reference gas analyzer running in parallel, we arbitrarily selected the data from the first hour of the second day (24 h period) after the sensors were installed to obtain a calibration reference from the FMA at the beginning of the season. The same was done at the end of the season, using the hour starting 24 h before the end of deployment to obtain a final calibration point.

Before we applied the calibration points to remove the linear trend from our data, we investigated time lags between the TGS 2600 sensor and the FMA reference. Although it is very clear that the TGS 2600 has a slower response than the FMA, we could not find a consistent and relevant time lag to be considered in such a calibration approach.

The real seasonal trend measured (under absence of instrument drift) by the FMA during almost 9 weeks of deployment was 0.00563 ppm week^{-1}, whereas our sensors 1 and 2 (including the respective sensor drift) had 0.0156 and 0.0140 ppm week^{-1}, respectively. This indicates that the trend in sensor signals increased above the real seasonal trend by 0.010 and 0.008 ppm week^{-1}, which must be taken in account if it is not possible to obtain an initial and a terminal calibration point over a period of deployment of a TGS 2600.

Table 1. Analysis of variance of the CH_4 sensor resistance R_s/R_0 for Toolik Lake, summer 2011.

Source of variation	Df	Sum Sq	Mean Sq	F value	Pr ($>F$)	Expl. Variance
Time trend	1	2825.29	2825.29	252 590	$< 2.2 \times 10^{-16}$***	36.1%
Relative humidity	1	1668.82	1668.82	149 198	$< 2.2 \times 10^{-16}$***	21.3 %
Methane concentration	1	1409.8	1409.8	126 041	$< 2.2 \times 10^{-16}$***	18.0 %
Air temperature	1	996.4	996.4	89 081	$< 2.2 \times 10^{-16}$***	12.7 %
Residual variation	82 976	928.11	0.01			11.9 %
Total	82 980	7828.42				100.0 %

Including this correction for the trend based on a calibration at the beginning ($[CH_4]_{raw,1}$ and $[CH_4]_{ref,1}$) and at the end ($[CH_4]_{raw,2}$ and $[CH_4]_{ref,2}$) of a deployment period, the final corrected TGS 2600 concentration $[CH_4]_{corr}$ becomes:

$$[CH_4]_{corr} = [CH_4]_{raw} + \left(1 - \frac{t}{\Delta t}\right) \cdot \left([CH_4]_{ref,1} - [CH_4]_{raw,1}\right) + \left(\frac{t}{\Delta t}\right) \cdot \left([CH_4]_{ref,2} - [CH_4]_{raw,2}\right), \quad (6)$$

where t is the elapsed time since the initial calibration time point, and Δt is the time difference between the terminal calibration and the initial calibration in the same time units.

3.5 Comparison with reference instrument

After all corrections were applied, we obtained a relatively good agreement with our reference instrument for both sensors (Fig. 4). There was, however, one period starting around 28–29 June where both TGA 2600 sensors deviated consistently from the reference instruments for several days. Although this period may have been related to smoke from wildfires (even though no smoke was observed), it was also very cold at this time with the first relevant snow fall at Toolik and in large parts of Alaska (Angeloff et al., 2011).

In the second part of the season, both TGA 2600 sensors closely followed the reference concentrations, albeit with a certain reduction in peak concentrations compared to the reference measurements; the most notable of these deviations occurred 27 and 28 July, and 3, 10, and 14 August (Fig. 4). Although the general information on the seasonal and diurnal patterns in CH_4 can be seen in Fig. 4, the pairwise agreement of all data points from the TGA 2600 with the reference concentration is only $R^2 = 0.195$ and 0.191, respectively, for sensors 1 and 2. This low statistical agreement can be misleading because the general diurnal pattern of CH_4 was quite accurately resolved (Fig. 5), both in terms of change over time and absolute concentrations. A fast Fourier transform (FFT) analysis of the frequency dependence of the performance of the TGA 2600 in relation to the reference instrument (Fig. 6) indicates that variations in methane occurring at a frequency lower than once per 6 h are captured rather well, whereas variations that occur at frequencies greater than once per hour are only partially captured (≈ 50 %) by the TGA 2600. Hence, in principle the diurnal cycle should be resolvable despite the fact that we only were able to obtain good agreement for average diurnal cycles obtained over many days, not for individual days. The systematic deviations between instruments seen on some days (Fig. 4) tend to show a slightly earlier timing of the early morning peak, a less steep decrease in concentrations during the morning until 9 h ADT, and a surprising daily minimum around 21 h ADT for the TGA sensors. This was not simply a time lag due to a long hysteresis of the TGA sensors. In fact, Ferri et al. (2009b) found a relatively fast time response for a TGS 2600 probed with step-changes in H_2 concentrations, to which the sensor reacted within a few minutes (their Fig. 11). The fact that we were unable to resolve individual diurnal cycles reflects the present limitations of the low-cost TGS 2600 sensor for more detailed studies, while showing that the sensors can still capture the essential pattern of diurnal changes in CH_4 concentrations. We also assume that if the airflow into the TGA 2600 was not passive but instead pumped (as was done with the LGR), the resolution of signals at higher frequencies would improve, especially at times when wind speeds are low.

4 Discussion

Because smoke is associated with high levels of CO to which the TGS 2600 is sensitive according to Figaro (2005a), there is some risk of confounding effects in areas where wildfire or other burning is present. However, during summer 2011, it appears that the uncertainty of the behavior of the TGS 2600 at cold temperatures (around freezing and below) led to the largest discrepancies with the reference concentration measurements. At least there were no reports of smoke or related odors at the site during this period. Morsi (2007) even claim that the TGS 2600 sensor is sensitive to CO_2, whereas the manufacturer does not mention a sensitivity for CO_2. They however do not explain why and how this sensor should respond to CO_2, but if this were true, it would seriously limit the usefulness of the application of the TGS 2600 for CH_4 measurements. To test for this potential limitation, we performed an additional ANOVA that included our

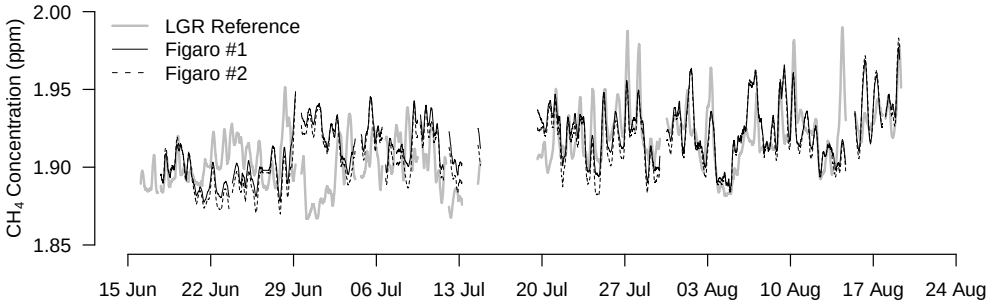

Fig. 4. Seasonal course of CH_4 concentration measurements over Toolik Lake during the ice-free season 2011. Data from all sensors where smoothed with a 6-h boxcar moving average.

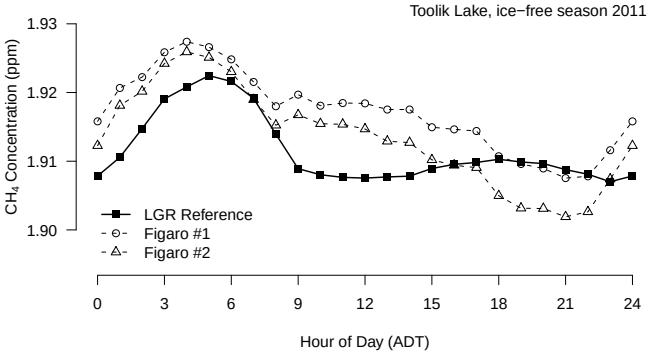

Fig. 5. Mean diurnal cycle of CH_4 concentrations over Toolik Lake during the ice-free season 2011. One-minute averages were aggregated by hour of day (Alaska Daylight Time). The standard error of the mean is of the same size as the symbol and hence is not added to the graph. The two low-cost sensors compare well with the Los Gatos Research reference analyzer during the first part of the day and correctly reflect the daily peak concentrations in the near-surface atmosphere.

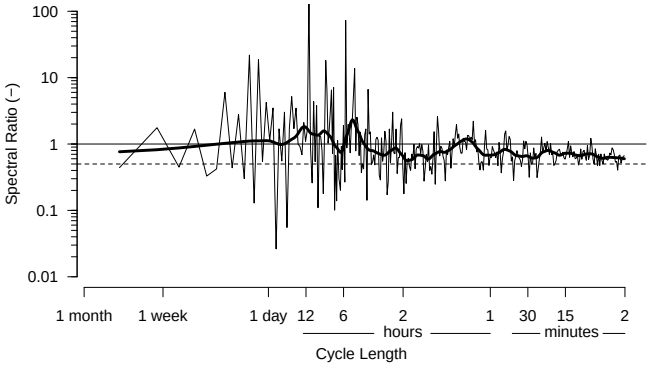

Fig. 6. Spectral densities of solid-state sensor #2 standardized by those measured by the Los Gatos Research reference analyzer during the longest period without data gaps (30 July to 14 August 2011). Calibrated data aggregated to 1-min averages were fast Fourier transformed, then bin-averaged to 200 bins of equal width on the log frequency axis, and then expressed as a ratio. The bold line is a local polynomial regression fit (loess function in *R* with $\alpha = 0.12$; $N = 22\,142$). Frequencies are labeled with their respective cycle lengths. At cycle lengths < 1 h, the solid-state sensor still captures more than 50% (dashed line) of the variance of the reference instrument. At cycle lengths > 6 h, a relatively good agreement was found.

CO_2 concentration measurements that were performed with a closed-path Li-7000 infrared gas analyzer (Licor, Lincoln, NE, USA) and atmospheric pressure. Table 2 summarizes the results which clearly show that CO_2 concentrations do not seriously affect the sensor's sensitivity for CH_4; the explained variance is 18 % and perfectly matches the result in the ANOVA without CO_2 (Table 1). Also, the relative humidity interference (21.1 % instead of 21.3 %) and the residual (unexplained) variance (11.8 % instead of 11.9 %) are only marginally affected by CO_2. The 3.5 % variance explained by CO_2 concentrations is thus simply reducing the explained variance of the temporal trend (strong reduction) and of temperature (an increase from 12.7 % to 18.0 %). Our interpretation is that this is a purely statistical artifact because (1) CO_2 has its own seasonal trend which is, however, negative over the summer season and more in agreement with the sensor drift that we quantified for the TGS 2600, and (2) the diurnal CO_2 cycle more strongly follows the diurnal temperature signal since both plant assimilation and respiration are correlated with temperature; given this, the changes in explained variances in Table 2 are likely unrelated to a cross-sensitivity of the TGS 2600 as was mentioned by Morsi (2007) but not by the manufacturer (Figaro, 2005a).

Although CO_2 concentration by itself does not appear to be of concern for CH_4 measurements with the TGS 2600, there is typically a tight correlation between CO_2 and CO concentrations if they come from combustion sources. Figure 1a from Figaro (2005a) indicates that the sensor's sensitivity to CO is similar to that of CH_4 for concentrations < 2–3 ppm. While this is the typical range for ambient CH_4 concentrations, the CO concentrations range between 0.03 and 0.2 ppm (Singh, 1995, p. 22) but can be up to 0.2–0.8 ppm in urban areas during summer months (Singh, 1995). At Point Barrow, which can be considered the best comparison with

Table 2. Same analysis as in Table 1, but with the inclusion of CO_2 concentrations and atmospheric pressure as a potential source of variation.

Source of variation	Df	Sum Sq	Mean Sq	F value	Pr ($> F$)	Expl. Variance
Time trend	1	2158.31	2158.31	193 894	$< 2.2 \times 10^{-16}$***	27.6 %
Relative humidity	1	1653.44	1653.44	148 539	$< 2.2 \times 10^{-16}$***	21.1 %
Methane concentration	1	1409.80	1409.80	126 651	$< 2.2 \times 10^{-16}$***	18.0 %
Air temperature	1	1407.83	1407.83	126 473	$< 2.2 \times 10^{-16}$***	18.0 %
CO_2 concentration	1	272.37	272.37	24 469	$< 2.2 \times 10^{-16}$***	3.5 %
Air pressure	1	3.05	3.05	273	$< 2.2 \times 10^{-16}$***	0.04 %
Residuals	82 974	923.61	0.01			11.8 %
Total	82 980	7828.41				100.0 %

Toolik Lake, Cavanagh et al. (1969) found about 0.09 ppm CO, which is far below the concentrations that would require a more careful consideration of CO as a confounding gas for the TGS 2600 measurements. In urban areas, however, a careful assessment would be needed to establish that the TGS 2600 primarily responds to CH_4 and not more strongly to CO.

Other substances that influence the TGS 2600 readings (Fig. 1a) are iso-butane, ethanol, and hydrogen. Iso-butane (R-600a) is an artificial refrigerant (C_4H_{10}) that is not expected to pose a serious problem for measurements at remote sites. Similarly, ethanol (C_2H_6O) is expected to have extremely low concentrations in the atmosphere because it is so highly soluble in water. Hydrogen (H_2) is present at 0.6 ppm in the average atmosphere (Singh, 1995), but the sources are mostly anthropogenic and likely can be ignored in the remote arctic tundra. Also, the effect of variations in atmospheric pressure were negligible (Table 2).

Error propagation from inaccurate temperature and relative humidity measurements does not strongly affect CH_4 concentration calculations. A systematic error of temperature readings offset by ± 4 K or relative humidity offset by 5 % only marginally affects CH_4 concentrations by less than 0.002 ppm. The reason is that the calibration step (Sect. 3.4) is the last in the processing chain, and any systematic error introduced in the preconditioning of the raw CH_4 signal is corrected within error margins that are clearly below the systematic uncertainty of the solid-state gas sensor. Random errors in temperature and relative humidity measurements are slightly more important; the accuracies of ± 0.4 K for temperature and ± 2 % for relative humidity in the typical ambient environment as specified by the manufacturer (see Section 2.3) lead to a mean error of 0.002 ppm and a 95% confidence interval of 0.002 to 0.003 ppm. This influence increases to 0.01 to 0.02 ppm for ± 4 K and ± 5 % uncertainties. This is still less than the remaining uncertainty that we found in the final solid-state sensor values which lay within ± 0.062 ppm (95 % confidence interval) of the reference instrument. Extreme differences were -0.15 and $+0.10$ ppm. Although apparently small, these errors are on the same order as the mean diurnal cycle shown in Fig. 5. Depending on objectives for deployment of these sensors, a careful consideration must be given to possible shortcomings in using a low-cost sensor as compared to a high-accuracy instrument. On the other hand, knowing the temporal dynamics, even at lower accuracy, may still provide additional insights as compared to the passive samplers described by Godbout et al. (2006a,b). It should also be mentioned that others (e.g., So et al., 2009) try to combine the aspect of economic costs with high-accuracy in a different way.

5 Conclusions

We tested a low-cost solid-state gas sensor (TGS 2600 from Figaro) for its suitability to measure ambient air concentrations of CH_4 in the low arctic at Toolik Lake in Alaska, USA, during the ice-free summer season of 2011. Two sensors were run in parallel and compared against a high-quality, off-axis integrated cavity output spectrometer (FMA, Los Gatos Research). The TGS 2600 revealed a high sensitivity for relative humidity and temperature similar to that expected from the specifications by the manufacturer. After corrections for these sensitivities, we obtained a realistic CH_4 signal that has the quality for preliminary studies to inspect temporal patterns of CH_4 concentrations, which could then inform the decision on whether a considerably more expensive instrument should be deployed for high-accuracy concentration measurements. One realistic approach would be to install such low-cost sensors in a regular grid with ≈ 1 km spacing to cover a landscape of interest, which could identify times, duration, and approximate locality of hotspots at the landscape scale.

In the seasonal average the TGS 2600 provided realistic insight into the temporal dynamics of CH_4 over Toolik Lake and also reproduced the average diurnal cycle of CH_4 with an early morning concentration peak of the correct order of magnitude at approximately the correct time of day. Both the general behavior and the systematic differences from the reference instrument were similar for the TGS sensors. From this experience we suggest that the TGS 2600 can be used for

preliminary assessment of CH_4 concentrations at sites where other gas components to which the sensor is sensitive are absent or at low concentrations, and where relative humidity is typically $> 40\,\%$. Such conditions are not only found in the low arctic, but also in rural areas of more populated zones where the distance to local CO sources can be substantial.

Acknowledgements. We acknowledge support received from the Arctic LTER grant NSF-DEB-1026843 including supplemental funding from the NSF-NEON and OPP-AON programs. Gaius R. Shaver (MBL) is acknowledged for initiating the study and supporting our activities in all aspects. We also thank Peter Plüss (ETH Zurich), Jennifer Kostrzewski (University of Michigan) and Dustin Carroll for technical and field assistance, and Dan White (MBL) for logistical support with the boats.

Edited by: P. Werle

References

Angeloff, H., Moore, B., Fathauer, T., Prechtel, A., and Thoman, R.: Alaskan Weather, Weatherwise, 64, 68–69, 2011.

Brudzewski, K.: An attempt to apply Elman's neural-network to the recognition of methane pulses, Sensor. Actuat. B-Chem., 47, 231–234, doi:10.1016/S0925-4005(98)00028-8, 1998.

Cavanagh, L. A., Schadt, C. F., and Robinson, E.: Atmospheric hydrocarbon and carbon monoxide measurements at Point Barrow, Alaska, Environ. Sci. Technol., 3, 251–257, 1969.

De Marcellis, A., Di Carlo, C., Ferri, G., Stornelli, V., Depari, A., Flammini, A., and Marioli, D.: New low-voltage low-power current-mode resistive sensor interface with R/T conversion and DC excitation voltage, in: Proceedings of the 13th Italian Conference On Sensors and Microsystems, 515–520, 2009.

DelSontro, T., McGinnis, D. F., Sobek, S., Ostrovsky, I., and Wehrli, B.: Extreme methane emissions from a Swiss hydropower reservoir: contribution from bubbling sediments, Environ. Sci. Technol., 44, 2419–2425, doi:10.1021/es9031369, 2010.

Dzikowski, M., Klyashitsky, A., Jaeger, W., and Tulip, J.: Open path spectroscopy of methane using a battery operated vertical cavity surface-emitting laser system, Proc. SPIE, 7386, 73861H, doi:10.1117/12.839519, 2009.

Efron, B.: Bootstrap methods: another look at the jackknife, The Annals of Statistics, 7, 1–26, 1979.

Eugster, W. and Plüss, P.: A fault-tolerant eddy covariance system for measuring CH_4 fluxes, Agr. Forest Meteorol., 150, 841–851, doi:10.1016/j.agrformet.2009.12.008, 2010.

Eugster, W., Kling, G., Jonas, T., McFadden, J. P., Wüest, A., MacIntyre, S., and Chapin III, F. S.: CO_2 exchange between air and water in an arctic Alaskan and midlatitude Swiss lake: importance of convective mixing, J. Geophys. Res., 108, 4362–4380, doi:10.1029/2002JD002653, 2003.

Eugster, W., McFadden, J. P., and Chapin III, F. S.: Differences in surface roughness, energy, and CO_2 fluxes in two moist tundra vegetation types, Kuparuk Watershed, Alaska, USA, Arct. Antarct. Alp. Res., 37, 61–67, 2005.

Eugster, W., DelSontro, T., and Sobek, S.: Eddy covariance flux measurements confirm extreme CH_4 emissions from a Swiss hydropower reservoir and resolve their short-term variability, Biogeosciences, 8, 2815–2831, doi:10.5194/bg-8-2815-2011, 2011.

Ferri, G., De Marcellis, A., Di Carlo, C., Stornelli, V., Flammini, A., Depari, A., Marioli, D., and Sisinni, E.: A CCII-based low-voltage low-power read-out circuit for DC-excited resistive gas sensors, IEEE Sens. J., 9, 2035–2041, doi:10.1109/JSEN.2009.2033197, 2009a.

Ferri, G., Di Carlo, C., Stornelli, V., De Marcellis, A., Flammini, A., Depari, A., and Jand, N.: A single-chip integrated interfacing circuit for wide-range resistive gas sensor arrays, Sensor. Actuat. B-Chem., 143, 218–225, doi:10.1016/j.snb.2009.09.002, 2009b.

Figaro: TGS 2600 – for the detection of air contaminants, Online product data sheet, http://www.figarosensor.com/products/2600pdf.pdf (last access: March 2012), 2005a.

Figaro: Technical information on usage of TGS sensors for toxic and explosive gas leak detectors, Online product information sheet, http://www.figarosensor.com/products/common%281104%29.pdf (last access: March 2012), 2005b.

Folorunso, O. A. and Rolston, D. E.: Spatial variability of field-measured denitrification gas fluxes, Soil Sci. Soc. Am. J., 48, 1214–1219, 1984.

Forster, P., Ramaswamy, V., Artaxo, P., Berntsen, T., Betts, R., Fahey, D. W., Haywood, J., Lean, J., Lowe, D. C., Myhre, G., Nganga, J., Prinn, R., Raga, G., Schulz, M., and Dorland, R. V.: Changes in atmospheric constituents and in radiative forcing, Cambridge University Press, 129–234, 2007.

Gibson, G., van Well, B., Hodgkinson, J., Pride, R., Strzoda, R., Murray, S., Bishton, S., and Padgett, M.: Imaging of methane gas using a scanning, open-path laser system, New J. Phys., 8, 26, 1–8, doi:10.1088/1367-2630/8/2/026, available at: http://www.njp.org/, 2006.

Godbout, S., Phillips, V. R., and Sneath, R. W.: Passive flux samplers to measure nitrous oxide and methane emissions from agricultural sources, Part 1: Adsorbent selection, Biosyst. Eng., 94, 587–596, doi:10.1016/j.biosystemseng.2006.04.014, 2006a.

Godbout, S., Phillips, V. R., and Sneath, R. W.: Passive flux samplers to measure nitrous oxide and methane emissions from agricultural sources, Part 2: Desorption improvements, Biosyst. Eng., 95, 1–6, doi:10.1016/j.biosystemseng.2006.05.007, 2006b.

Haifang, L., Shisheng, Z., Rui, W., and Keqiang, L.: Remote helicopter-borne laser detector for searching of methane leak of gas line, in: Prognostics and System Health Management Conference (PHM2011 Shenzhen), MU3049, 2011.

Hiller, R., Neininger, B., Brunner, D., Buchmann, N., and Eugster, W.: Aircraft-based methane flux estimates for an agriculturally dominated valley in Switzerland, Geophysical Research Abstracts, 13, EGU2011-7015-1, 2011.

Karapuzikov, A., Ponomarev, Y., Ptashnik, I., Romanovsky, O., Kharchenko, O., and Sherstov, I.: Helicopter lidar project for the remote methane leakage detection based on the TEA CO_2 laser radiation harmonics, in: Science and Technology, 1999, KORUS '99, Proceedings, The Third Russian-Korean International Symposium on, Vol. 2, 663–666, doi:10.1109/KORUS.1999.876253, 1999.

Kotarski, M., Smulko, J., Czyzewski, A., and Melkonyan, S.: Fluctuation-enhanced scent sensing using a single gas sensor, Sensor. Actuat. B-Chem., 157, 85–91, doi:10.1016/j.snb.2011.03.029, 2011.

MacIntyre, S., Fram, J. P., Kushner, P. J., Bettez, N. D., O'Brien, W. J., Hobbie, J. E., and Kling, G. W.: Climate-related variations in mixing dynamics in an Alaskan arctic lake, Limnol. Oceanogr., 54, 2401–2417, 2009.

McGuire, A. D., Chapin, III, F. S., Walsh, J. E., and Wirth, C.: Integrated regional changes in arctic climate feedbacks: Implications for the global climate system, Annu. Rev. Environ. Resour., 31, 61–91, doi:10.1146/annurev.energy.31.020105.100253, 2006.

Morsi, I.: A microcontroller based on multi sensors data fusion and artificial intelligent technique for gas identification, Iecon 2007: 33rd Annual Conference of the IEEE Industrial Electronics Society, Vol. 1–3, Conference Proceedings, 2203–2208, doi:10.1109/IECON.2007.4460098, 2007.

Morsi, I.: Electronic noses for monitoring environmental pollution and building regression model, Iecon 2008: 34th Annual Conference of the IEEE Industrial Electronics Society, Vol. 1–5, Proceedings, 1668–1673, 2008.

R Development Core Team: R: A Language and Environment for Statistical Computing, R Foundation for Statistical Computing, Vienna, Austria, http://www.R-project.org, ISBN 3-900051-07-0, 2010.

Reeburgh, W. S., King, J., Regli, S., Kling, G., Auerbach, N., and Walker, D.: A CH_4 emission estimate for the Kuparuk River Basin, Alaska, J. Geophys. Res., 103, 29005–29013, 1998.

Schmid, H. P.: Source areas for scalars and scalar fluxes, Bound.-Lay. Meteorol., 67, 293–318, 1994.

Schroth, M. H., Eugster, W., Gómez, K. E., Gonzalez-Gil, G., Niklaus, P. A., and Oester, P.: Above- and below-ground methane fluxes and methanotrophic activity in a landfill-cover soil, Waste Manage., 5, 879–889, doi:10.1016/j.wasman.2011.11.003, 2012.

Serreze, M. C. and Francis, J. A.: The arctic amplification debate, Clim. Change, 76, 241–264, doi:10.1007/s10584-005-9017-y, 2006.

Singh, H. B. (Ed.): Composition, Chemistry, and Climate of the Atmosphere, Van Nostrand Reinhold, New York, 527 pp., 1995.

So, S., Sani, A. A., Zhong, L., Tittel, F., and Wysocki, G.: Laser spectroscopic trace-gas sensor networks for atmospheric monitoring applications, in: Proceedings of the 8th ACM/IEEE International Conference on Information Processing in Sensor Networks, vol. ESSA 2009, 1–8, 2009.

Tümer, A. E. and Gündüz, M.: Design of a methane monitoring system based on wireless sensor networks, Sci. Res. Essays, 5, 799–805, 2010.

Tuzson, B., Hiller, R. V., Zeyer, K., Eugster, W., Neftel, A., Ammann, C., and Emmenegger, L.: Field intercomparison of two optical analyzers for CH_4 eddy covariance flux measurements, Atmos. Meas. Tech., 3, 1519–1531, doi:10.5194/amt-3-1519-2010, 2010.

Walter, K. M., Zimov, S. A., Chanton, J. P., Verbyla, D., and Chapin III, F. S.: Methane bubbling from Siberian thaw lakes as a positive feedback to climate warming, Nature, 443, 71–75, doi:10.1038/nature05040, 2006.

Werle, P.: Time domain characterization of micrometeorological data based on a two sample variance, Agric. Forest Meteorol., 150, 832–840, doi:10.1016/j.agrformet.2009.12.007, 2010.

Wong, K. K. L., Tang, Z. A., Sin, J. K. O., Chan, P. C. H., Cheung, P. W., and Hiraoka, H.: Sensing mechanism of polymer for selectivity enhancement of gas sensors, ICSE '96 – 1996 IEEE International Conference On Semiconductor Electronics, Proceedings, 217–220, doi:10.1109/SMELEC.1996.616485, 1996.

Zirnig, W., Ulbricht, M., Fix, A., and Klingenberg, H.: Helicopter-borne laser methane detection system – a new tool for efficient gas pipeline inspection, in: International Gas Research Conference, Vancouver, Canada, 2004.